Multiplicity Features of Adiabatic Autothermal Reactors

Marianne Lovo and Vemuri Balakotaiah
Dept. of Chemical Engineering, University of Houston, Houston, TX 77204

Singularity theory, large activation energy asymptotics, and numerical methods are used to present a comprehensive study of the steady-state multiplicity features of three classical adiabatic autothermal reactor models: tubular reactor with internal heat exchange, tubular reactor with external heat exchange, and the CSTR with external heat exchange. Specifically, we derive the exact uniqueness-multiplicity boundary, determine typical cross-sections of the bifurcation set, and classify the different types of bifurcation diagrams of conversion vs. residence time. Asymptotic (limiting) models are used to determine analytical expressions for the uniqueness boundary and the ignition and extinction points. The analytical results are used to present simple, explicit and accurate expressions defining the boundary of the region of autothermal operation in the physical parameter space.

Introduction

Autothermal processes allow the heat of reaction to be utilized in such a way to maintain a temperature high enough for the reaction to occur without any heat or fuel source once the reaction is started. In autothermal processes, unlike many other reacting systems, the existence of multiple steady states is to be maintained rather than avoided. This is because these reactors usually operate on the upper or ignited steady state. Some well known examples of processes carried out in autothermal reactors are the synthesis of ammonia, methanol and hydrogen. There are three configurations that are commonly used for autothermal operation: a tubular reactor with internal heat exchange, a tubular reactor with an external heat exchanger, and a continuous flow stirred tank reactor with an external heat exchanger. In each of these arrangements, the heat of combustion is used to preheat the incoming feed to the required temperature at which the reaction occurs. This is accomplished via countercurrent heat exchange of the hot product stream and the ambient feed stream.

There have been extensive studies of adiabatic autothermal reactors in the literature (Van Heerden, 1953, 1958; Baddour et al., 1965; Ampaya and Rinker, 1977a,b; Inoue and Komiya, 1968, 1978; Mukosei et al., 1968). Van Heerden (1953) first investigated the steady-state behavior of an autothermal tubular reactor with internal heat exchange using the ammonia synthesis reactor as an example. He also investigated autothermic processes in which a feedback of heat resulted in the possibility of multiple steady states. An adiabatic CSTR (continuously stirred tank reactor), a plug flow reactor with external heat exchange, and a tubular reactor with heat dispersion were considered (van Heerden, 1958). The conditions under which autothermal operation is feasible were determined either graphically or numerically for all three reactor models. Mukosei et al. (1968) also investigated the steady-state regimes of tubular reactors with internal, external and combined heat exchange. Inoue and Komiya (1968) and Ampaya and Rinker (1977a) investigated the stability of a tubular reactor with internal heat exchange with regard to the critical feed temperature for several different operating and design parameters. Inoue and Komiya (1968) developed conditions for the stable operation of the autothermal reactor for both reversible and irreversible reactions. They include approximate analytical criteria for predicting both ignition and extinction points as well as the critical stable point (cusp point). The results of this method are only qualitative and are useful in predicting the qualitative effect of varying parameters on the stability of the reactor. Ampaya and Rinker (1977a) adopted a similar approach and related the critical feed temperature (at extinction) to various operating and design parameters for the case of the water-gas shift reaction. Later, conditions for reactor runaway were also developed by Inoue (1978). Strictly speaking, reactor runaway is not an issue in the operation of autothermal reactors. The concept of reactor runaway, however, is related closely to the question of reactor ignition and the presence of multiple steady states. Hence, the use of these concepts allows

the determination of regions where multiple solutions are possible and therefore allows the determination of the region of autothermal operation.

Although many previous studies have examined the existence of these multiple steady states and the stability of the reactor, there exist no simple, accurate and explicit criteria for predicting the conditions under which autothermal operation is feasible. The goal of this work is to present a comprehensive analysis of the steady-state behavior of the three classical adiabatic autothermal reactor models: a tubular reactor with internal heat exchange, a tubular reactor with external countercurrent heat exchange, and a CSTR with an external heat exchanger. We use the singularity theory, shooting technique and large activation energy asymptotics and various limiting cases to analyze the steady-state behavior of these three models. By combining these techniques, we develop simple analytical expressions for the uniqueness boundary and the ignition and extinction points.

Autothermal Tubular Reactor with Internal Heat Exchange

Mathematical model and method of solution

We consider the case of an autothermal reactor with negligible heat and mass dispersion with a first-order irreversible reaction $A \rightarrow B$. The downtube (inner or preheating tube) of the reactor is used as the preheat zone, and the reaction occurs in the uptube (outer or reaction tube) of the reactor. The resulting steady-state model is given by:

$$\frac{dy_d}{d\xi} = St(y_u - y_d) \tag{1}$$

$$\frac{dy_u}{d\xi} = -\beta Da(1-\chi)\exp\{\gamma y_u/(1+y_u)\} + St(y_u - y_d) \tag{2}$$

$$\frac{d\chi}{d\xi} = -Da(1-\chi)\exp\{\gamma y_u/(1+y_u)\} \tag{3}$$

with boundary conditions

$$\chi(\xi=1)=0;\ y_d(\xi=1)=y_u(\xi=1);\ y_d(\xi=0)=0, \tag{4}$$

where

$$y=\frac{T-T_o}{T_o} \quad \chi=\frac{c_{A0}-c_A}{c_{A0}} \quad \xi=\frac{x}{L}$$

$$\gamma=\frac{E}{RT_o} \quad \beta=\frac{(-\Delta H_r)c_{A0}}{T_o\rho_f C_{pf}}$$

$$Da=\frac{k(T_o)V_r}{q} \quad St=\frac{UA_h}{\rho_f C_{pf} q} \tag{5}$$

Here, y_d and y_u are the nondimensional temperatures in the downtube (preheat section) and uptube (reactor section), respectively. χ is the conversion of species A, and ξ represents axial position along the reactor ($\xi=0$ represents the inlet of the preheat section at the top of the reactor, and $\xi=1$ the inlet of the reaction section at the bottom). The four parameters are: γ, the dimensionless activation energy; β, the adiabatic temperature rise which is proportional to the heat of reaction and inlet concentration; Da, the Damkohler number that is proportional to the residence time; St, the Stanton number that is a measure of the heat transfer between the tubes.

The two energy balance equations (Eqs. 1-2) may be combined to eliminate y_u. The resulting equations for y_d and χ are:

$$\frac{d^2y_d}{d\xi^2} + \beta StDa(1-\chi)\exp\left\{\frac{\gamma\left(y_d+\frac{1}{St}\frac{dy_d}{d\xi}\right)}{1+y_d+\frac{1}{St}\frac{dy_d}{d\xi}}\right\}=0 \tag{6}$$

$$\frac{d\chi}{d\xi} + Da(1-\chi)\exp\left\{\frac{\gamma\left(y_d+\frac{1}{St}\frac{dy_d}{d\xi}\right)}{1+y_d+\frac{1}{St}\frac{dy_d}{d\xi}}\right\}=0 \tag{7}$$

$$\chi(\xi=1)=0; \quad y_d(\xi=0)=0; \quad \frac{dy_d}{d\xi}(\xi=1)=0. \tag{8}$$

Equations 6-8 may be combined to obtain an invariant:

$$\chi(\xi)=\frac{1}{\beta St}\frac{dy_d}{d\xi}. \tag{9}$$

Substitution of Eq. 9 into Eq. 6 gives a single second-order differential equation for y_d. For convenience, we drop the subscript and refer to y_d as y:

$$\frac{d^2y}{d\xi^2} + \beta St\,Da\exp\left\{\frac{\gamma\left(y+\frac{1}{St}\frac{dy}{d\xi}\right)}{1+y+\frac{1}{St}\frac{dy}{d\xi}}\right\}\left(1-\frac{1}{\beta St}\frac{dy}{d\xi}\right)=0 \tag{10a}$$

$$y(0)=0, \quad y'(1)=0. \tag{10b}$$

The boundary value problem described by Eq. 10 may be converted to an initial value problem by using the shooting technique. Denoting the bottom temperature $y(1)$ as t, the initial conditions are:

$$y(1)=t$$

$$\frac{dy}{d\xi}(1)=0. \tag{11}$$

We then integrate backwards using a standard initial value package, iterating on the value of t to satisfy the steady-state equation for the boundary condition at $\xi=0$:

$$f(t,Da,St,\gamma,\beta)\equiv y(0,t)=0. \tag{12}$$

By treating the problem in this manner, the solution of the infinite dimensional problem is reduced to that of solving a single algebraic equation with a single state variable, which is

the temperature at the bottom of the reactor. Accordingly, we can apply the results of singularity theory of a single state variable to examine the bifurcation behavior and multiplicity features (Balakotaiah and Luss, 1984; Witmer et al., 1986). This requires generating additional variational equations along with the appropriate boundary conditions for the singular points (for details see Witmer et al., 1986; Lovo, 1991). We use the shooting method in conjunction with the arclength continuation scheme described by Kubicek and Marek (1983) to construct the bifurcation diagrams as well as the locus of the limit points and cusp points.

We assume that the steady-state equation (Eq. 12) satisfies the conditions set forth by Balakotaiah and Luss (1984). The bifurcation set (locus of ignition and extinction points) is defined by Eq. 12 and

$$\frac{df}{dt}=0. \tag{13}$$

Elimination of t between Eqs. 12 and 13 gives the bifurcation set in the (Da,St,γ,β) space. The ignition and extinction loci coalesce at the cusp point. The cusp point is defined by Eqs. 12 and 13, and

$$\frac{d^2f}{dt^2}=0. \tag{14}$$

Elimination of t and Da from Eqs. 12–14 gives the exact uniqueness-multiplicity boundary in the (St,γ,β) space: that is, on one side of this boundary a unique solution exists for all Da, while on the other side multiple solutions may exist for some range of Da values.

In practice, it is of interest to know the different types of bifurcation diagrams that describe the state variable (t) as a function of an operating variable (residence time, feed temperature, or concentration). In this study, we are interested in the flow rate, or equivalently the residence time as the bifurcation variable. In Eq. 10, the residence time appears in two dimensionless groups (Da,St). Accordingly, we reparameterize the steady-state equation (Eq. 12) such that the residence time appears only in the Damkohler number. We define a new dimensionless group, H, which is independent of residence time and rewrite:

$$St=H\,Da \tag{15a}$$

$$H=\frac{UA_h}{\rho_f C_{pf} k(T_o) V_r}. \tag{15b}$$

The steady-state equation (Eq. 12) is now rewritten as:

$$\hat{f}(t,Da,H,\gamma,\beta)\equiv y(0,t)=0. \tag{16}$$

The procedure for computing the bifurcation set (limit points) and uniqueness-multiplicity boundary (hysteresis points) is the same as described above.

Determination of uniqueness-multiplicity boundary

Since it is desirable to operate an autothermal reactor at an ignited steady state, it is useful then to know for what ranges of parameter values γ,β and St (or H) an ignited steady state can exist. Alternatively, for a given activation energy, heat of reaction and heat transfer coefficient, one would like to calculate the critical inlet concentration below which autothermal operation cannot be sustained. Figure 1 shows bifurcation diagrams of the exit conversion vs. the Damkohler number for fixed values of the Stanton number and the activation energy. Curve (a) shows that for small values of β, the conversion is a unique and monotonically increasing function of the Damkohler number. Moreover, we observe that the conver-

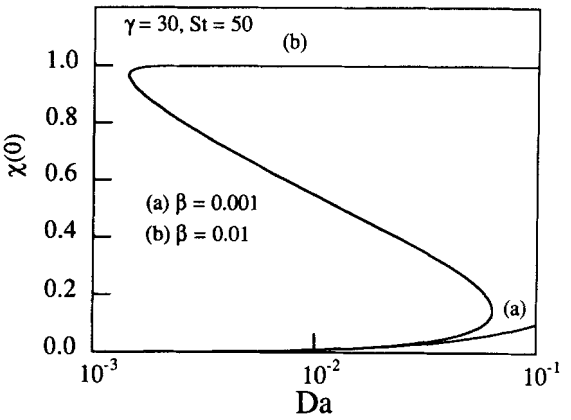

Figure 1. Bifurcation diagrams of exit conversion vs. Damkohler number for different values of β.

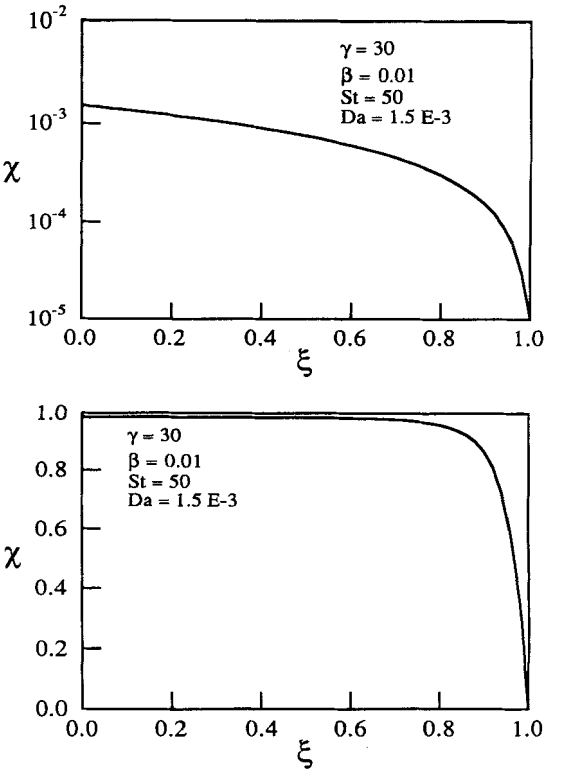

Figure 2. Conversion profiles along the reactor for the extinguished and ignited steady states corresponding to $Da=1.5E\text{-}3$ on Figure 1, curve (b).

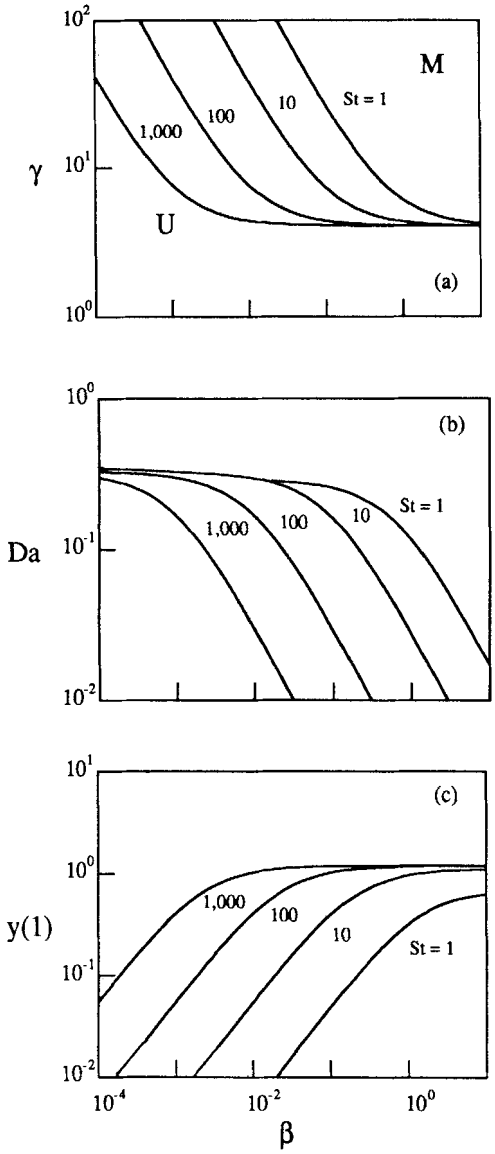

Figure 3. Exact uniqueness-multiplicity boundary projected in the (γ,β), (Da,β), and [$y(1),\beta$] plane.

U denotes uniqueness; *M* denotes multiplicity.

sions for this case are very small. Curve (b) shows that for larger values of β, multiple steady states exist for a range of Da. The bifurcation diagram for case (b) exhibits a hysteresis (s-shape) behavior with an ignited high-conversion steady state and an extinguished low-conversion steady state. Figure 2 shows the conversion profiles for an extinguished and an ignited steady state corresponding to the same Damkohler number on curve (b) of Figure 1. In practice, it is the high-conversion steady state which is of interest. To determine for what set of parameters multiple steady states are possible, we calculate the uniqueness-multiplicity boundary or the cusp locus using singularity theory as described above.

Figures 3a to 3c show the cusp locus for various Stanton numbers projected in the (γ,β), (Da,β) and [$y(1),\beta$] planes. For (γ,β) values above the curves in Figure 3a, three solutions are possible for some range of Da values. Below the curves, a unique solution is guaranteed regardless of the value of Da.

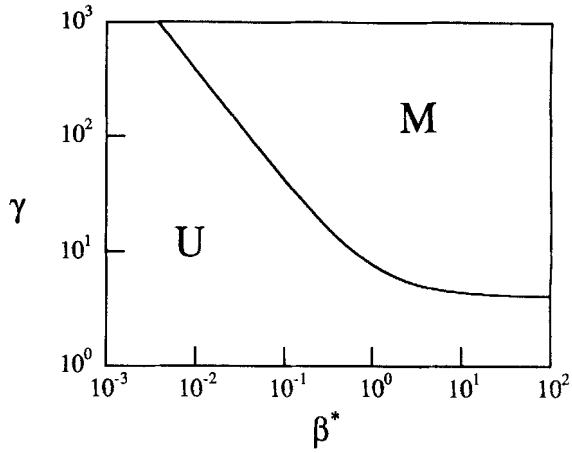

Figure 4. Exact uniqueness-multiplicity boundary for the high heat transfer model (HHTUMB) in the (γ,β^*) space.

U denotes uniqueness; *M* denotes multiplicity.

We observe that the curves are described by two distinct asymptotes. For large values of β, the cusp locus approaches a horizontal asymptote at a constant value of γ and $y(1)$, while the product βDa remains finite. For small values of β, the uniqueness boundary approaches another asymptote for which the Damkohler number and the products $\gamma\beta$ and $\gamma y(1)$ approach constant values. By defining $\beta^* = \beta St$ and replotting the results, we also observe a third limiting model for large values of Stanton number. The uniqueness-multiplicity boundary in the (γ,β^*) plane becomes independent of St and may be expressed by a single curve shown in Figure 4. (The curves for $St = 10$, 100 and 1,000 are indistinguishable on the scale used in Figure 4). We now examine each of these limiting models.

High heat transfer model: ($St >> 1$, $\beta << 1$, βSt finite)

We shall refer to the limiting curve shown in Figure 4 as the "high heat transfer uniqueness-multiplicity boundary" (HHTUMB). The limiting model defining this boundary may be obtained by taking $St >> 1$, $\beta << 1$ and $\beta St = \beta^*$ in Eq. 10. The resulting model is given by:

$$\frac{d^2y}{d\xi^2} + Da\left(\beta^* - \frac{dy}{d\xi}\right)\exp\left\{\frac{\gamma y}{1+y}\right\} = 0 \tag{17}$$

$$y = 0; \quad \xi = 0 \tag{18a}$$

$$\frac{dy}{d\xi} = 0; \quad \xi = 1 \tag{18b}$$

This model contains only three parameters (γ, β^*, and Da). Figure 4 shows the numerically computed exact U-M boundary of this model. The cusp locus of this model is characterized by two distinct asymptotes. For $\beta^* << 1$, the cusp locus approaches the asymptote $\gamma\beta^* = 3.777$, $Da = 0.3223$, $\gamma y(1) = 2.165$. For $\beta^* >> 1$, the cusp locus approaches the asymptote $\gamma = 4.068$, $\beta^* Da = 0.3213$, $y(1) = 1.203$.

Positive exponential approximation model: ($\beta << 1$, $\gamma >> 1$, $\gamma\beta$ finite)

The results for low β values in Figure 3 show that the product $\gamma\beta^*$ approaches a constant value which depends on the Stanton number. In analogy with the CSTR, we assume that the temperature $y_u(1)$ is small compared to unity so that the positive exponential approximation may be used. Defining

$$\theta = \gamma y, \quad B^* = \gamma\beta^*, \tag{19}$$

the limiting model is given by:

$$\frac{d^2\theta}{d\xi^2} + Da(B^* - \theta')\exp\left\{\theta + \frac{\theta'}{St}\right\} = 0 \tag{20}$$

$$\theta = 0; \quad \xi = 0 \tag{21a}$$

$$\frac{d\theta}{d\xi} = 0; \quad \xi = 1. \tag{21b}$$

Figure 5 shows the computed values of B^*, Da and $\theta(1)$ at the cusp point as a function of the Stanton number. Here, we observe that as St becomes large, the cusp point becomes independent of the Stanton number. This corresponds to the low β^* asymptote of the HHTUMB, in which we showed that for high heat transfer, the U-M boundary in the (γ,β) plane is independent of the Stanton number. Thus, for low β^* and large St values, we can further simplify the above model by dropping the term θ'/St in the exponent of Eq. 20. The resulting model contains only two parameters, B^* and Da. Numerical calculations show that it has a single cusp point at:

$$\theta(1) = 2.165; \quad B^* = 3.777; \quad Da = 0.3223. \tag{22}$$

Negligible reactant consumption model: ($Da << 1$, $\beta >> 1$, βDa finite)

The asymptote corresponding to large β may be obtained by neglecting reactant consumption. This simplifies Eq. 10 to:

$$\frac{d^2y}{d\xi^2} + \delta\exp\left\{\gamma\left(y + \frac{y'}{St}\right)\Big/\left(1 + y + \frac{y'}{St}\right)\right\} = 0 \tag{23}$$

$$y = 0; \quad \xi = 0 \tag{24a}$$

$$\frac{dy}{d\xi} = 0; \quad \xi = 1 \tag{24b}$$

where

$$\delta = \beta StDa. \tag{25}$$

This model contains only three parameters (δ, γ, and St). Thus, for each St number, we can find the values of δ and γ at the cusp point. Figure 6 shows plots of γ, δ and $y(1)$ at the cusp point for various Stanton numbers. In the limit that St becomes large, we observe the HHTUMB asymptote ($St >> 1$, $\beta >> 1$). In this case, we neglect the terms y'/St in the exponent of Eq. 23. This is the negligible reactant consumption limit of the high heat transfer model described in Eqs. 17 and 18. This model contains only two parameters, (γ and δ) and has a single cusp point (Eaton and Gustafson, 1983) at:

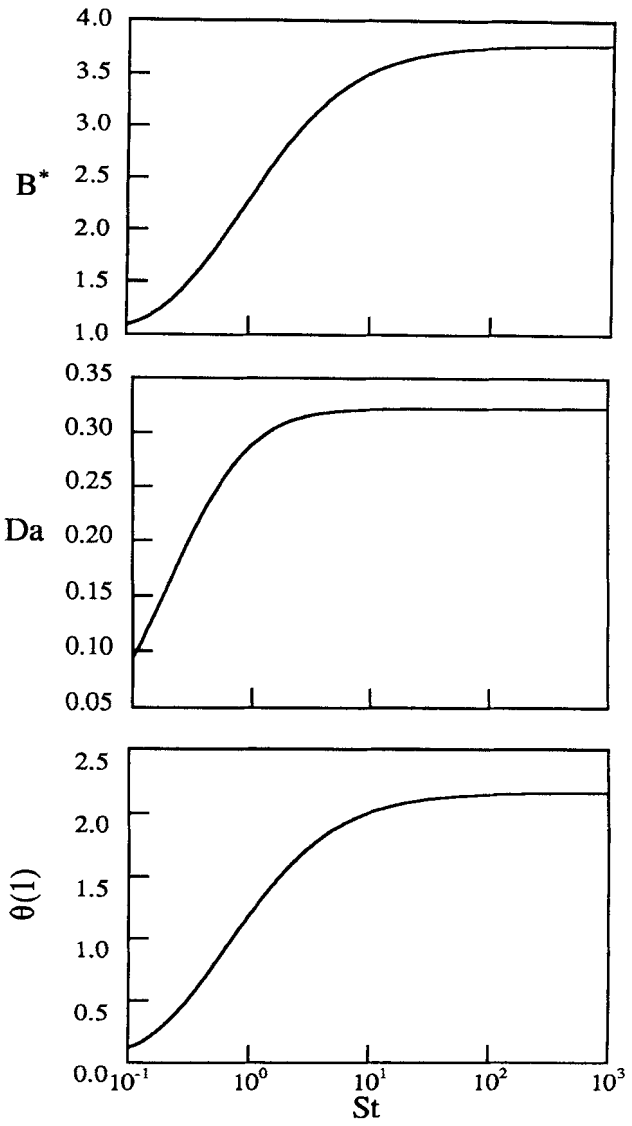

Figure 5. Dependence of B^*, Da, and $\theta(1)$ at the cusp point on the Stanton number for the positive exponential approximation model.

$$\gamma = 4.068; \quad \delta = \beta^* Da = 0.3213; \quad y(1) = 1.203. \tag{26}$$

Results with residence time as bifurcation variable

It is also of interest to examine the uniqueness multiplicity boundary in the (γ,β,H) space. In this formulation, the flow rate or equivalently the residence time is isolated in the Damkohler number. Figure 7 shows the cusp locus for various values of H in the (γ,β) plane. Above the curves, three solutions are possible for some range of Da or residence time. Below the curves, there is a unique solution for all values of the residence time. In the case of $\beta << 1$, we observe the same type of behavior as in the previous formulation: $\gamma\beta H$ approaches a constant value. The product $\gamma\beta H$ also becomes

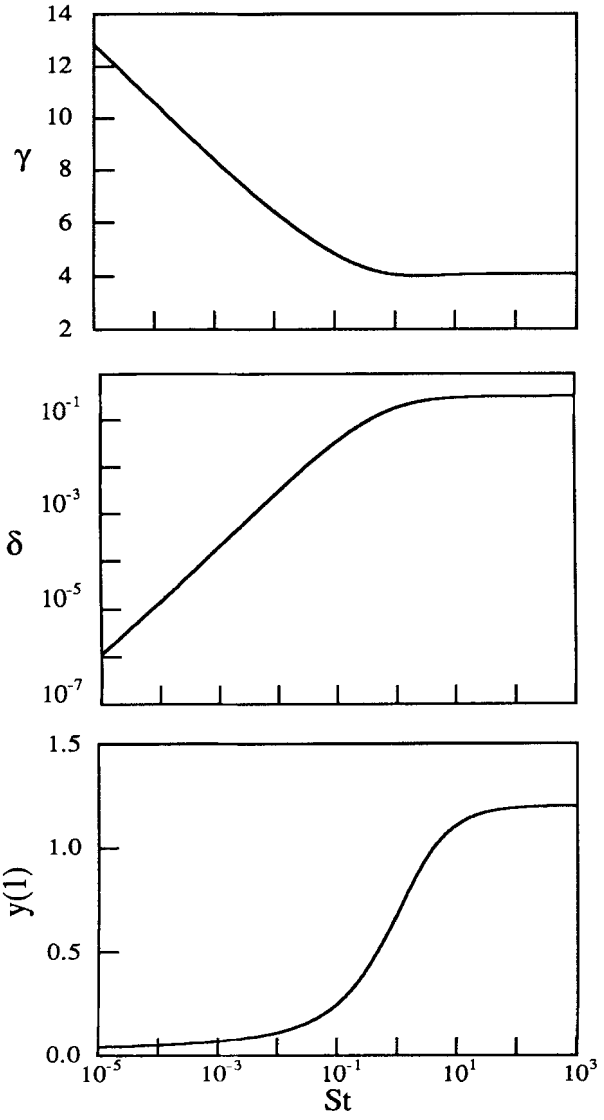

Figure 6. Dependence of γ, y and δ at the cusp point on the Stanton number for the negligible reactant consumption model.

independent of H for large values of H. However, for the case $\beta >> 1$, the curves do not level off at a constant value of γ. To understand these results we examine the reparameterized cusp locus for the two limiting cases of the positive exponential approximation model and the negligible reactant consumption model.

Here, we describe both the asymptotes by the same limiting models simply substituting HDa for the Stanton number. Accordingly, we reparameterize the results shown in Figures 5 and 6. For $\beta << 1$, we keep Da intact and define the following groups:

$$\gamma\beta H = \frac{B^*}{Da}$$

$$H = \frac{St}{Da}. \tag{27}$$

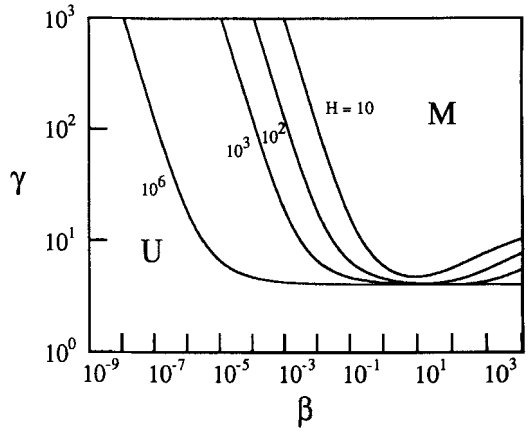

Figure 7. Exact uniqueness-multiplicity boundary in the (γ,β) space for different values of H.

For the case of $\beta >> 1$, we reparameterize the problem, leaving γ intact and define the groups:

$$\beta Da = \frac{\delta}{St}$$

$$\frac{\beta}{H} = \frac{\delta}{St^2}. \tag{28}$$

We show the reparameterized plots of cusp points for the limiting cases of positive exponential approximation model

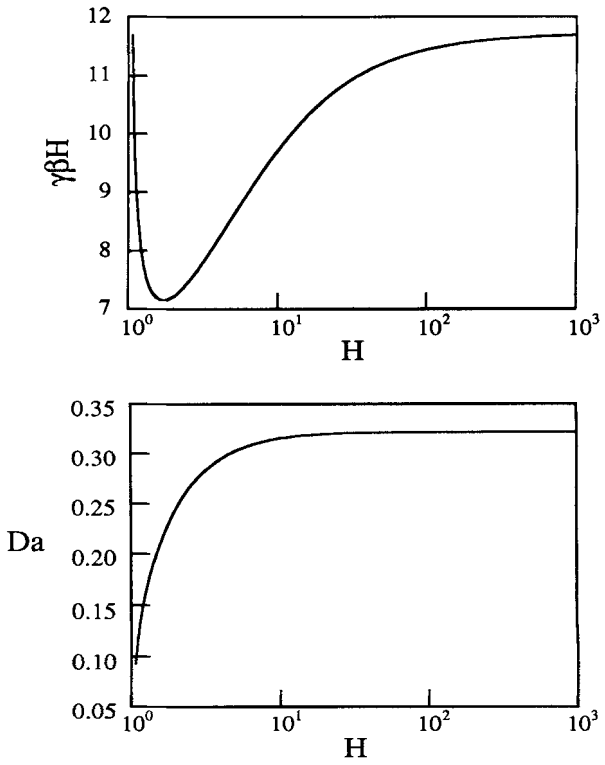

Figure 8. Dependence of $\gamma\beta H$ and Da at the cusp point on H for the positive exponential approximation model.

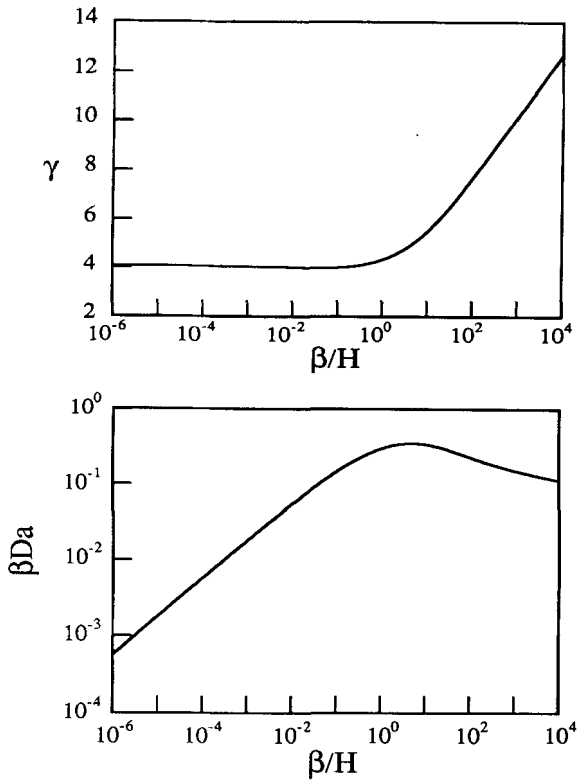

Figure 9. Dependence of γ and βDa and at the cusp point on β/H for the negligible reactant consumption model.

($\beta << 1, \gamma >> 1, \gamma\beta$ finite) and the negligible reactant consumption model ($\beta >> 1, Da << 1, \beta Da$ finite) in Figures 8 and 9.

For the small β asymptote, the results are analogous to those for the Stanton formulation with H replacing the Stanton number. In Figure 8, we show the values of $\gamma\beta H$ and Da at the cusp point for various H values. For large H, the value of $\gamma\beta H$ becomes independent of H. We find this limit from the result of Eq. 22 by using the reparameterized groups defined in Eq. 27:

$$\gamma\beta H = 11.722 \tag{29}$$

We also observe that both curves have a vertical tangent at $H=1$ and that cusp points occur only for $H>1$.

For the case of the large β (negligible reactant consumption asymptote), we examine the results shown in Figure 9. The value of the cusp point for this asymptote depends on the ratio of β/H. Since we are plotting the cusp points in the (γ,β) plane, this ratio changes constantly along the β axis. For the case that β/H is small, we see the same asymptote of $\gamma=4.068$ as in the previous formulation, but as this ratio becomes large the value of γ at the cusp increases. This explains the behavior observed in Figure 7 in which the upward turn of the curve occurs at larger values of β for larger values of H. Although the curve for $H=10^6$ appears to level off, the curve turns upwards at higher values of β. Only in the limit $H=\infty$ and $\beta \neq \infty$, there is a horizontal asymptote at $\gamma=4.068$.

The two asymptotes defined above for $\beta << 1$ and $\beta >> 1$ provide an excellent approximation of the uniqueness-multiplicity boundary for autothermal reactors. In practice, β^* is much smaller than unity so that the asymptote defined by Eq. 22 provides the required approximation for the exact uniqueness-multiplicity boundary. We note that the low β^* asymptote of the HHTUMB provides an exact boundary for uniqueness-multiplicity in the case that the Stanton number is large and a conservative prediction for multiplicity in the case that the Stanton number is small. That is, if the values of γ and β^* are such that they lie above this boundary, then autothermal operation is possible for some range of Damkohler numbers. For the reparameterized problem, in which residence time is the bifurcation variable, we note that Eq. 29 defines the conditions for autothermal operation. By examining Figure 8, we observe that this is an exact criterion for large H and a conservative boundary for multiplicity when H is small. We note the exception for the region near $H=1$. However, typical values of H do not fall in this region. Therefore, for all practical cases in which $H>100$, we can define a general criterion for autothermal operation as

$$\gamma\beta H > 11.722 \tag{30a}$$

or in terms of physical parameters,

$$\frac{E}{RT_o}\frac{(-\Delta H_r)c_{A0}}{\rho_f C_{pf} T_o}\frac{UA_h}{\rho_f C_{pf} k(T_o) V_r} > 11.722. \tag{30b}$$

If Eq. 30 is satisfied, an ignited steady state exists for some range of residence times. On the other hand, when Eq. 30 is not satisfied, autothermal operation is too feeble to maintain an ignited steady state for any reactor length or flow rate.

Determination of bifurcation set (ignition and extinction locus)

The cusp locus determined in the previous section is useful for determining for a given system (characterized by γ, β and H or St) whether multiplicity is possible for some range of Damkohler numbers or equivalently residence times. However, if we are interested in determining for what Damkohler numbers or residence times these multiple solutions occur, we must examine the bifurcation sets (or equivalently, the locus of ignition and extinction points). The bifurcation set for the full mathematical model is a surface in the four dimensional space (γ, β, St, and Da). Here, we present cross-sections of the bifurcation set in the (St,Da) space for typical values of γ and β. Since we are interested in cases where γ is large and β is small, it follows that St at the cusp is large. We note that in this case, we may simplify the determination of the bifurcation set by eliminating an additional parameter (St) by considering the high heat transfer model described by Eqs. 17-18. This model is defined by the parameters (γ, β^*, and Da). Figure 10 shows a cross section of the bifurcation set for the high heat transfer model in the ($\beta^* - Da$) plane for $\gamma=30$, along with two cases for the full model for $\beta=0.1$ and $\beta=0.01$. For the case of $\beta=0.1$, we see that there is a slight discrepancy near the region of the cusp point, but otherwise the ignition and extinction points predicted by the high heat transfer model are very close to those of the full model. For the case of $\beta=0.01$, the two curves are almost indistinguishable. Although the bi-

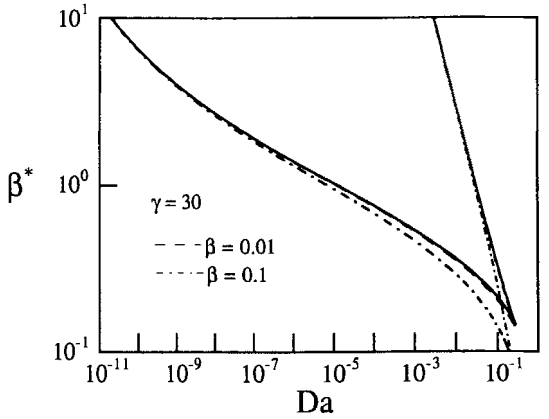

Figure 10. Cross-section of the bifurcation set in the (β^*,*Da*) plane for the high heat transfer model and the full model.

furcation set for the high heat transfer model depends on fewer parameters, it must be computed numerically for each activation energy of interest. We attempt to develop, therefore, analytical approaches so that one can easily and accurately determine the ignition and extinction points.

Prediction of ignition points (Frank-Kamenetskii model)

We can determine the ignition locus analytically by assuming negligible reactant consumption and by using the positive exponential approximation. The resulting model follows from Eqs. 20 and 21 by neglecting reactant consumption.

$$\frac{d^2\theta}{d\xi^2} + \Delta e^{\theta} = 0 \tag{31}$$

$$\theta = 0; \quad \xi = 0 \tag{32a}$$

$$\frac{d\theta}{d\xi} = 0; \quad \xi = 1, \tag{32b}$$

where

$$\Delta = \gamma\beta StDa. \tag{33}$$

This is the classical Frank-Kamenetskii thermal explosion model (Frank-Kamenetskii, 1969). This model has an ignition point at

$$\Delta = 0.8785, \quad \theta(1) = 1.187. \tag{34}$$

Prediction of extinction points

For the determination of extinction points, we are not able to make any simplifying assumptions. However, we are able to simplify the task of finding the extinction points by treating the problem in the following manner. We integrate Eq. 9 over the length of the reactor to obtain a relationship between bottom temperature and exit conversion $\chi_e = \chi(0)$:

$$y(1) = \beta^* \chi_e. \tag{35}$$

In addition, we assume that for the case of high heat transfer, the reaction occurs in a very small portion of the reactor (point source) and the reactor tubes act only as the heat exchanger. Thus, the temperature in the reactor can be approximated by the linear profile:

$$y(\xi) = \beta^* \chi_e \xi. \tag{36}$$

The steady-state equation is obtained by integrating the mass balance. Thus, the ignited steady states are described by the equation:

$$F(\chi_e, \gamma, \beta^*, Da) = Da - g(\chi_e, \gamma, \beta^*) = 0, \tag{37}$$

where

$$g(\chi_e, \gamma, \beta^*) = \frac{-\ln(1-\chi_e)}{\int_0^1 \exp[\gamma(\beta^*\chi_e\xi)/(1+\beta^*\chi_e\xi)]d\xi}. \tag{38}$$

We note that $g(0) = 0$ and $g(1) = \infty$, and g is a single valued function of χ_e. For large values of γ ($\gamma > 20$), an excellent approximation of the function $g(\chi_e)$ is given by:

$$g(\chi_e, \gamma, \beta^*) = \frac{\gamma\beta^*\chi_e \ln\left(\frac{1}{1-\chi_e}\right) \exp\left\{\frac{-\gamma\beta^*\chi_e}{1+\beta^*\chi_e}\right\}}{(1+\beta^*\chi_e)^2}. \tag{39}$$

The extinction point of this model is defined by the minimum of the above function. It may be obtained by the simultaneous solution of Eqs. 37 and 39 and

$$\frac{dg}{d\chi_e} = 0. \tag{40}$$

It is not possible to obtain an explicit analytical expression for the extinction locus. However, we can express the locus in a parametric form:

$$\beta^* \equiv G(\chi_e, \gamma) \tag{41a}$$

$$Da = g[\chi_e, \gamma, G(\chi_e, \gamma)], \quad (0 < \chi_e < \chi_e^*), \tag{41b}$$

where χ_e^* is defined by:

$$B(\chi_e^*)^2 - 4C(\chi_e^*) = 0 \tag{41c}$$

and

$$G(\chi_e, \gamma) = \frac{B(\chi_e) \pm \sqrt{B(\chi_e)^2 - 4C(\chi_e)}}{2\chi_e C(\chi_e)} \tag{41d}$$

$$A(\chi_e) = 1 + \frac{\chi_e}{(1-\chi_e)\ln\left(\frac{1}{1-\chi_e}\right)} \tag{41e}$$

$$B(\chi_e) = \frac{\gamma+2}{A(\chi_e)} - 2 \tag{41f}$$

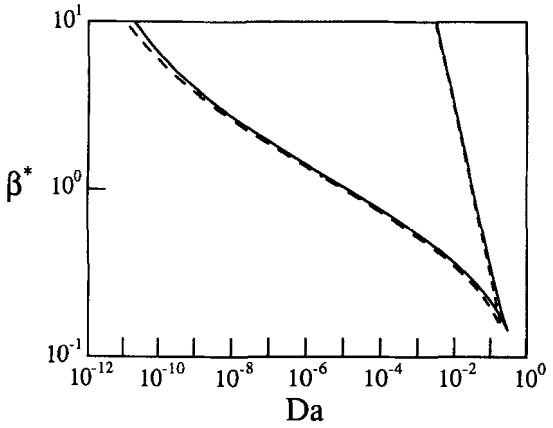

Figure 11. Cross-section of the bifurcation set in (β^*,*Da*) plane for the high heat transfer model compared with analytical expressions for the ignition and extinction points (dashed curves) for $\gamma = 30$.

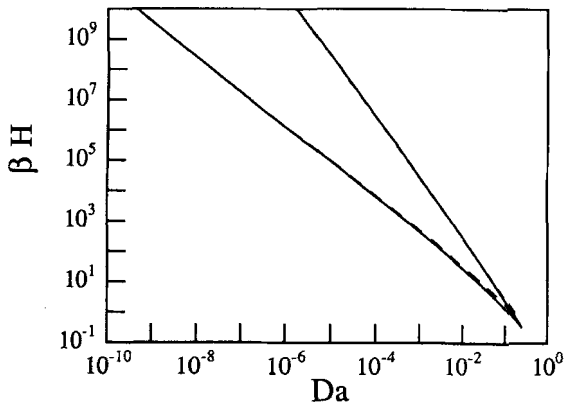

Figure 12. Cross-section of the bifurcation set in the (βH,*Da*) plane for the full model ($\gamma = 30$ and $\beta = 0.1$) and the analytical expressions for the ignition and extinction points (dashed curves).

$$C(\chi_e) = 1 - \frac{2}{A(\chi_e)}. \tag{41g}$$

We note that the conversion is nonmonotonic along the extinction branch. The lower portion of the extinction branch is described by Eq. 41*d* with the negative sign. At the critical value, χ_e^*, the discriminant becomes zero and the conversion reaches a maximum. The extinction branch is then defined by Eq. 41*d* with the positive sign. Figure 11 shows the approximated bifurcation set along with the numerically calculated bifurcation set for the high heat transfer model. We observe that these approximations describe the bifurcation set very accurately. Therefore, in the cases where the heat transfer is high (almost all practical cases), these approximations may be used to determine the ignition and extinction points.

Results with residence time as bifurcation variable

Above, we considered cross-sections of bifurcation sets in the (*St-Da*) or equivalently (β^*-*Da*) plane. We note, however, that the residence times at the ignition and extinction points in terms of H, γ and β can be determined from these diagrams. This can be done by using the bifurcation set in the (β^*,*Da*) plane and following lines of constant slope ($= \beta H$). Along these lines, β^* and *Da* change linearly with the residence time. Therefore, following these lines of constant slope corresponds to increasing the Damkohler number in the reparameterized problem. The intersection of these lines with the bifurcation set in the (β^*,*Da*) plane gives the ignition and extinction points. The approximate expressions derived above may be rewritten to obtain the residence times at ignition and extinction:

$$Da_{ig} = \left(\frac{0.8785}{\gamma\beta H}\right)^{0.5} \tag{42}$$

$$(\beta H)_{ext} = \frac{G(\chi_e,\gamma)}{g[\chi_e,\gamma,G(\chi_e,\gamma)]} \tag{43a}$$

$$Da_{ext} = g[\chi_e,\gamma,G(\chi_e,\gamma)], \tag{43b}$$

where $G(\chi_e,\gamma)$ is as defined in Eq. 41. Figure 12 shows the computed bifurcation set for the full model for $\gamma = 30$ and $\beta = 0.1$, along with the expressions given for predicting the ignition and extinction locus in Eqs. 42 and 43. Typical values of H are from 10^4 to 10^8. Again, we see that these analytical expressions approximate the bifurcation set extremely well.

Tubular Reactor with External Heat Exchange

Tubular reactors often utilize external rather than internal heat exchange to achieve autothermal operation. In this case, the products and reactant are passed through a countercurrent heat exchanger which is external to the reactor. The autothermal reactor with external heat exchange is described by the following mathematical model. The reactor is described by the plug flow model:

$$\frac{dy}{d\xi} = \beta Da(1-\chi)\exp\{\gamma y/(1+y)\} \tag{44}$$

$$\frac{d\chi}{d\xi} = Da(1-\chi)\exp\{\gamma y/(1+y)\} \tag{45}$$

with boundary conditions

$$\chi(0) = 0; \quad y(0) = y_o. \tag{46}$$

The balance for the heat exchanger results in the following relationship between the reactor inlet and outlet, and the exit temperature of the heat exchanger y_e:

$$y(0) = Sty_e \tag{47}$$

$$y(1) = (1+St)y_e. \tag{48}$$

Combining Eqs. 44–48 gives the following steady-state equation for the exit temperature:

$$Da=\int_{Sty_e}^{(1+St)y_e}\frac{dy}{\exp\left(\frac{\gamma y}{1+y}\right)(\beta+Sty_e-y)}. \tag{49}$$

Determination of uniqueness-multiplicity boundary

The cusp locus of this model may be found using the singularity theory for a single algebraic equation (Balakotaiah and Luss, 1984). Figure 13 shows the uniqueness-multiplicity boundaries in the (γ,β^*) plane for various St numbers. We note that the same limiting models (high heat transfer, positive exponential approximation, and negligible reactant consumption) occur for both cases of internal and external heat exchange. Since we are generally interested in large values of the Stanton number, we focus on the results for the high heat transfer model. For this case, we can simplify Eq. 49 as:

$$Da=\exp\left(\frac{-\gamma Sty_e}{1+Sty_e}\right)\ln\left(\frac{\beta}{\beta-y_e}\right). \tag{50}$$

For convenience, we rewrite Eq. 50 substituting

$$Sty_e=\beta^*\chi=\beta St\chi, \tag{51}$$

where χ is the conversion of the reactant:

$$Da=\exp\left(\frac{-\gamma\beta^*\chi}{1+\beta^*\chi}\right)\ln\left(\frac{1}{1-\chi}\right). \tag{52}$$

We can find the cusp locus of this equation in a parametric form:

$$\beta^*=\frac{1+\ln(1-\chi)}{\left[(2-\chi)\ln\left(\frac{1}{1-\chi}\right)-\chi\right]}$$

$$\gamma=\frac{4(1-\chi)\ln\left(\frac{1}{1-\chi}\right)}{\left[(2-\chi)\ln\left(\frac{1}{1-\chi}\right)-\chi\right][1+\ln(1-\chi)]}$$

$$Da=\ln\left(\frac{1}{1-\chi}\right)\exp\left\{\frac{-2\chi}{(2-\chi)\ln(1-\chi)+\chi}\right\}\quad 0<\chi<1-e^{-1}. \tag{53}$$

For the low β^* asymptote ($\beta^*\to 0$), the steady-state equation simplifies to:

$$Da=-\exp(-\theta)\ln\left(1-\frac{\theta}{B^*}\right), \tag{54a}$$

where

$$\theta=\gamma Sty_e=\gamma\beta^*\chi$$

$$B^*=\gamma\beta^*. \tag{54b}$$

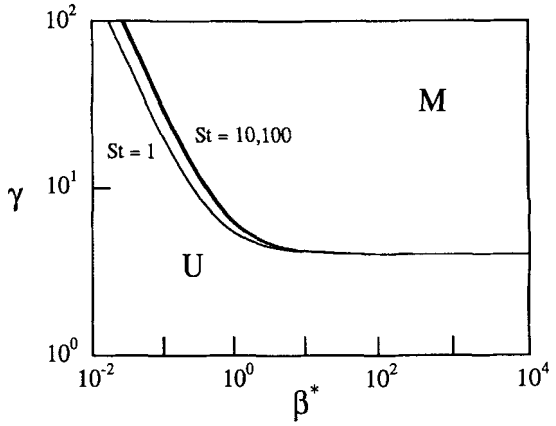

Figure 13. Exact uniqueness-multiplicity boundary in the (γ,β^*) space for different Stanton numbers for the autothermal tubular reactor with external heat exchange.

U denotes uniqueness; *M* denotes multiplicity.

The cusp point of this model is given by:

$$Da=e^{1-e},\quad \theta=e-1,\quad B^*=e. \tag{55}$$

For the case that residence time is taken as the bifurcation variable, we observe the following criterion for autothermal operation

$$\gamma\beta H>e^e=15.154, \tag{56a}$$

or in terms of physical parameters

$$\frac{E}{RT_o}\frac{(-\Delta H_r)C_{A0}}{T_o\rho_f C_{pf}}\frac{UA_h}{\rho_f C_{pf}k(T_o)V_r}>e^e=15.154. \tag{56b}$$

For the case of negligible reactant consumption, ($\beta^*>>1$, $Da<<1$), Eq. 52 simplifies to:

$$\beta^* Da=\exp\left\{\frac{-\gamma\beta^*\chi}{1+\beta^*\chi}\right\}\beta^*\chi. \tag{57}$$

The cusp point for this model is given by:

$$\beta^*\chi=1;\quad \gamma=4;\quad \beta^* Da=e^{-2}. \tag{58}$$

The asymptotes given by Eqs. 55 and 58 correspond to $\chi\to 1-e^{-1}$ and $\chi\to 0$, respectively, in Eq. 53.

Determination of ignition and extinction points

We can also determine the locus of ignition and extinction points for the high heat transfer model described by Eq. 52. The limit points of the high heat transfer model can be described in a parametric form by Eq. 52 and

$$\beta^*=\frac{f(\chi)-2\pm\sqrt{f(\chi)^2-4f(\chi)}}{2\chi}\quad 0<\chi<\chi^*, \tag{59a}$$

where

$$f(\chi)=\gamma\frac{(1-\chi)\ln\left(\frac{1}{1-\chi}\right)}{\chi} \tag{59b}$$

and χ^* is defined by

$$f(\chi^*)-4=0. \tag{59c}$$

We note that both the ignition and extinction points can be determined for the case of residence time as the bifurcation variable by substituting $\beta^*=\beta HDa$ into Eqs. 52 and 59.

Autothermal CSTR

We also compare the above results to those for an autothermal CSTR in which the effluent from the reactor is passed through a heat exchanger to preheat the feed. For this case, there is multiplicity even in the case that the Stanton number is zero. The conversion in an autothermal CSTR is given by:

$$\chi=Da(1-\chi)\exp\left(\frac{\gamma\hat{\beta}\chi}{1+\hat{\beta}\chi}\right), \tag{60}$$

where

$$\hat{\beta}=\beta(1+St) \tag{61a}$$

$$y=\hat{\beta}\chi, \quad St=HDa. \tag{61b}$$

Equation 60 is identical in form to that of the adiabatic CSTR with $\hat{\beta}$ playing the role of β. For the high heat transfer model ($St>>1$), we note that $\hat{\beta}\approx\beta^*$.

Determination of uniqueness-multiplicity boundary

In analogy with the case of the tubular reactor with both internal and external heat exchange, we investigate this model for the high heat transfer limit by replacing $\hat{\beta}$ with β^*. The cusp locus can be written in the following parametric form:

$$\gamma=\frac{2(y+1)}{y} \quad 0<y<1 \tag{62a}$$

$$\beta^*=\frac{2y}{1-y} \tag{62b}$$

$$Da=\frac{1-y}{1+y}e^{-2}. \tag{62c}$$

Elimination of y from Eqs. 62*a* and 62*b* gives an analytical expression for the uniqueness boundary in the (γ,β^*) plane $\gamma\beta^*/(1+\beta^*)=4$ (Aris, 1969). From Eq. 62, we observe the two asymptotes for the limits of small and large β^*. For $\beta^*<<1$ and $\gamma>>1$, or equivalently $y\to 0$, the cusp locus approaches the asymptote described by:

$$\gamma\beta^*=4; \quad \theta=\gamma y=2; \quad Da=e^{-2}. \tag{63}$$

For $\beta^*>>1$ and $Da<<1$, the cusp locus approaches the negligible reactant consumption asymptote:

$$\gamma=4; \quad \beta^*Da=e^{-2}; \quad y=1. \tag{64}$$

The criterion for autothermal operation for small β^* follows from Eq. 63. An ignited steady state is possible only if

$$\gamma\beta H>4e^2=29.556 \tag{65a}$$

or equivalently

$$\frac{E}{RT_o}\frac{(-\Delta H_r)C_{A0}}{T_o\rho_f C_{pf}}\frac{UA_h}{\rho_f C_{pf}k(T_o)V_r}>4e^2=29.556. \tag{65b}$$

While the CSTR exhibits multiple steady states even for $St=0$, a comparison of Eq. 65 with Eqs. 30 and 56 shows that for large St values it is more difficult to achieve autothermal operation with a CSTR than a tubular reactor with internal or external heat exchange.

Determination of ignition and extinction points

We can also determine the locus of ignition and extinction points analytically for the CSTR with external heat exchange. Again, we consider the case of high heat transfer. Analytical expressions for both the ignition and extinction points may be obtained by solving for

$$F=0, \quad \frac{dF}{d\chi}=0, \tag{66}$$

where F is the steady-state equation defined by Eq. 60 with β^* replacing $\hat{\beta}$. Differentiating F and substituting Eq. 60 give the following expression for the conversion at the ignition and extinction points:

$$\beta^*(\beta^*+\gamma)\chi^2+\beta^*(2-\gamma)\chi+1=0. \tag{67}$$

For each value of (γ,β^*), we may obtain the values of the conversion at the ignition and extinction points by solving for the roots, χ_c, of the above quadratic equation. The corresponding value of the Damkohler number at the limit point (ignition or extinction) may be obtained by substituting the values of γ,β^* and χ_c into the steady-state equation:

$$Da_c=\frac{\chi_c}{(1-\chi_c)}\exp\left(\frac{-\gamma\beta^*\chi_c}{1+\beta^*\chi_c}\right). \tag{68}$$

We can get a more explicit form for both the ignition and extinction points by making the standard approximations. For the ignition point, we use the positive exponential approximation. Since we are interested in the lower extinguished branch, we assume that reactant consumption is negligible or that $\chi<<1$ and define:

$$\theta=\gamma\beta^*\chi, \quad B^*=\gamma\beta^*. \tag{69}$$

The resulting steady-state equation is given by:

$$Da=\frac{\theta e^{-\theta}}{B^*}. \tag{70}$$

The ignition point of this equation is given by:

$$Da_{ig} = \frac{e^{-1}}{B^*}. \tag{71}$$

For the extinction point, we can simplify the analysis by using large activation energy asymptotics. The Damkohler number at the extinction point is given by:

$$Da_{ext} = \frac{\gamma\beta^* e}{(1+\beta^*)^2} \exp\left\{\frac{-\gamma\beta^*}{1+\beta^*}\right\}. \tag{72}$$

When the residence time formulation is used, Eq. 71 may be rearranged as:

$$Da_{ig} = \left(\frac{0.368}{\gamma\beta H}\right)^{1/2}. \tag{73}$$

The extinction point may be given in a parametric form given by Eq. 72 and

$$\beta H_{ext} = \frac{\beta^*}{Da_{ext}} = \frac{(1+\beta^*)^2}{\gamma e} \exp\left\{\frac{\gamma\beta^*}{1+\beta^*}\right\}. \tag{74}$$

Practical Criteria for Strong Autothermal Operation

In practice, autothermal reactors are operated on the ignited high-conversion branch at residence times that are slightly higher than at the extinction point. It is of interest to determine the critical flow rate and feed temperature (corresponding to the extinction point) as a function of the design parameters such as the adiabatic temperature, activation energy, and degree of preheating. This can be accomplished by rewriting the steady-state equations using the following substitutions:

$$\gamma = \frac{E}{RT_o} = \frac{E}{RT_R}\frac{T_R}{T_o} = \gamma_R y_R$$

$$\beta^* = \frac{\Delta T_{ad}}{T_o}\left(\frac{UA_h}{q\rho_f C_{pf}}\right) = \beta_R^* y_R$$

$$y_R = \frac{T_R}{T_o}; \quad \beta_R^* = \frac{\Delta T_{ad}}{T_R}\left(\frac{UA_h}{q\rho_f C_{pf}}\right)$$

$$T_R = T_o + \Delta T_{ad} St; \quad Da_R = \frac{V_r k(T_R)}{q}. \tag{75}$$

Here, $(T_R - T_o)$ is the maximum possible preheating of the reaction mixture. On the ignited branch where the conversion is close to unity, T_R is approximately equal to the reaction temperature. γ_R is the dimensionless activation energy at T_R, and β_R^* is the ratio of the preheating to T_R. Substitution of Eq. 75 into Eqs. 37 and 39, and dropping of the subscript e on χ_e gives:

$$Da_R = \frac{\gamma_R\beta_R^*\chi}{[1-\beta_R^*(1-\chi)]^2} \ln\left(\frac{1}{1-\chi}\right) \exp\left\{\frac{\gamma_R\beta_R^*(1-\chi)}{1-\beta_R^*(1-\chi)}\right\}. \tag{76}$$

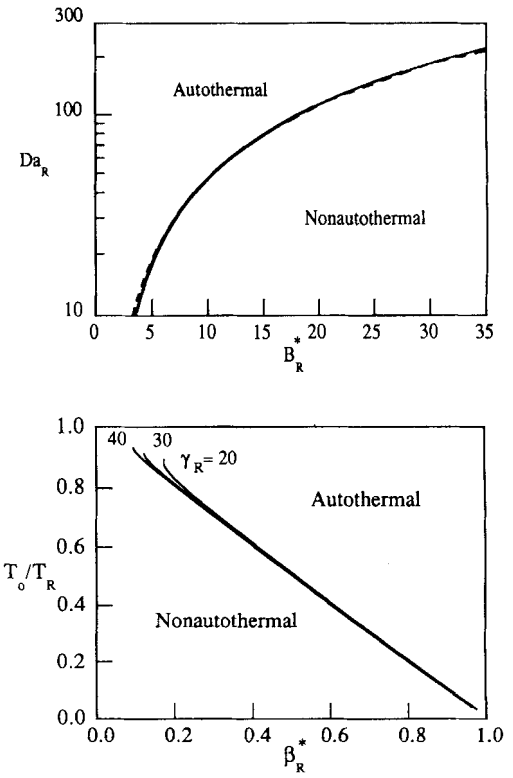

Figure 14. Boundaries of the region of autothermal operation for the tubular reactor with internal heat exchange.

The top diagram gives the critical flow rate and the bottom diagram gives the critical feed temperature.

Similarly, for the autothermal reactor with external heat exchange, we get:

$$Da_R = \ln\left(\frac{1}{1-\chi}\right) \exp\left\{\frac{\gamma_R\beta_R^*(1-\chi)}{1-\beta_R^*(1-\chi)}\right\}, \tag{77}$$

while for the CSTR,

$$Da_R = \left(\frac{\chi}{1-\chi}\right) \exp\left\{\frac{\gamma_R\beta_R^*(1-\chi)}{1-\beta_R^*(1-\chi)}\right\}. \tag{78}$$

Figures 14-16 show the extinction locus of each of the above three reactor models for typical values of $\gamma_R = 20$, 30 and 40. The curves for these three different values of γ_R are nearly coincident so that a single curve may be used to define the boundary of the region of parameters in which autothermal operation is feasible. We can further use large activation energy asymptotics to obtain simple and accurate expressions to describe these three curves. We make use of the fact that the conversion at the extinction point is close to unity so that the approximations,

$$\chi \approx 1 \quad \text{and} \tag{79a}$$

$$\beta_R^*(1-\chi) << 1, \tag{79b}$$

are valid. The steady-state equations (Eqs. 76-78) may now be simplified to:

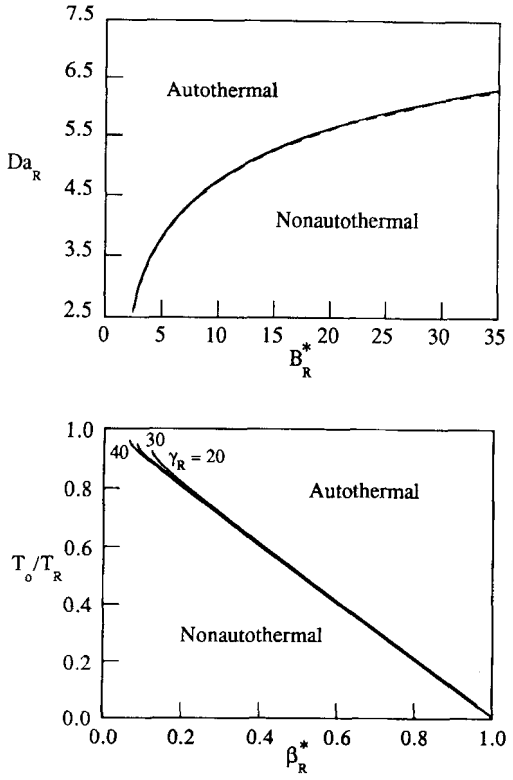

Figure 15. Boundaries of the region of autothermal operation for the tubular reactor with external heat exchange.

The top diagram gives the critical flow rate and the bottom diagram gives the critical feed temperature.

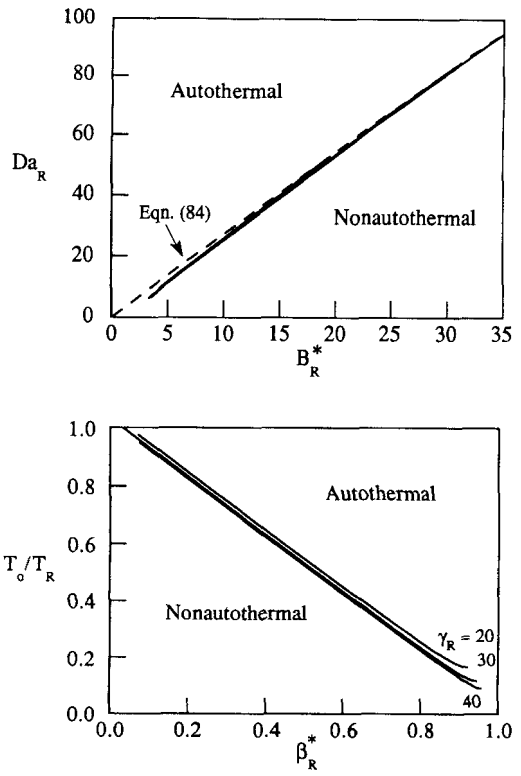

Figure 16. Boundaries of the region of autothermal operation for CSTR with external heat exchange.

The top diagram gives the critical flow rate and the bottom diagram gives the critical feed temperature.

$$Da_R = B_R^* e^{v} \ln\left(\frac{B_R^*}{v}\right) \quad \text{(internal heat exchange)} \tag{80a}$$

$$Da_R = e^{v} \ln\left(\frac{B_R^*}{v}\right) \quad \text{(external heat exchange)} \tag{80b}$$

$$Da_R = B_R^* \left(\frac{e^{v}}{v}\right) \quad \text{(CSTR with external heat exchange),} \tag{80c}$$

where

$$v = B_R^*(1-\chi) \tag{81a}$$

and

$$B_R^* = \gamma_R \beta_R^* = \frac{E}{RT_R} \cdot \frac{\Delta T_{ad}}{T_R} \cdot St \tag{81b}$$

For the autothermal reactor with internal heat exchange, the extinction locus is given in the following parametric form:

$$Da_R = \exp\left(v + \frac{1}{v}\right)$$

$$B_R^* = v \exp\left(\frac{1}{v}\right), \quad 0 < v < 1. \tag{82}$$

Similarly, for the case of external heat exchange, we can express the extinction locus in a parametric form:

$$Da_R = \frac{e^{v}}{v}$$

$$B_R^* = v \exp\left(\frac{1}{v}\right), \quad 0 < v < 1. \tag{83}$$

For the CSTR with external heat exchange, we are able to derive the following explicit criterion:

$$Da_R = B_R^* e. \tag{84}$$

When these analytical expressions are compared to the numerical results of the extinction points obtained from Eqs. 76-78 shown in Figures 14-16, the curves are essentially indistinguishable. We also note that all three of the curves of (T_o/T_R) vs. β_R^* intersect the ordinate near 1 and approach a slope of -1. We can see this result more easily by examining the relationship between y_R and β_R^*

$$\frac{1}{y_R} = 1 - \beta_R^* + \beta_R^*(1-\chi). \tag{85}$$

For conversions close to unity, Eq. 85 becomes:

$$\frac{T_o}{T_R} = 1 - \beta_R^*, \tag{86}$$

which is valid for all three reactor models. Thus, Eq. 86 may be used to estimate the critical feed temperature, while Eqs. 82-84 give the critical flow rate determining the boundary of the region of autothermal operation.

Conclusions

This work provides a comprehensive analysis of the multiplicity features of three classical adiabatic autothermal reactor models: tubular reactor with internal heat exchange, tubular reactor with external heat exchange, and the CSTR with external heat exchange. We analyzed the mathematical model using two different formulations. In the first case (Stanton formulation), the flow rate and reactor length enter in both the Stanton number and the Damkohler number. In the second case, the effect of flow rate or residence time is isolated in the Damkohler number.

Important results include the determination of the exact uniqueness-multiplicity boundary along with the two asymptotes of this boundary for $\beta << 1$ and $\beta >> 1$. For the first case (Stanton formulation), we observe a third limiting model for large Stanton that corresponds to high heat transfer in which the uniqueness-multiplicity boundary becomes independent of the Stanton number. Of particular interest to autothermal reactors is the asymptote for $\beta << 1$, or the case where inlet concentrations are small. For this case, we determined the criterion for autothermal operation (existence of multiple solutions for some range of residence times) to be $\gamma\beta H > 11.722$ (internal), 15.154 (external), and 29.556 (CSTR). Thus, we see that autothermal operation is the easiest to obtain for the tubular reactor with internal heat exchange and the most difficult to obtain for the CSTR.

The above expressions (based on the uniqueness-multiplicity boundary) provide a weak criteria for autothermal operation. That is, these conditions must be satisfied for the existence of an ignited steady state for some range of residence times. To determine the operating conditions needed to achieve strong autothermal operation, we derived the criteria (locus of extinction points) in terms of feed temperature and flow rate. We also expressed these in terms of the reaction temperature, instead of the feed temperature. This is useful as in many practical cases the reaction temperature is specified and reaction rate at this temperature is known. In this case, the criteria given by Eqs. 82-84 and 86 give the critical flow rate and critical feed temperature needed for the autothermal operation. The approach that we have developed can also be extended to determine both strong and weak criteria for autothermal operation for other types of kinetic expressions (nth-order reactions) as well as reversible reactions.

Acknowledgment

The research is supported by the Gulf Coast Hazardous Substances Research Center (GCHSRC), the American Chemical Society Petroleum Research Fund, and the Robert A. Welch Foundation.

Notation

A_h = heat exchange area

$B^* = \dfrac{E}{RT_o}\dfrac{\Delta T_{ad}}{T_o}\dfrac{UA_h}{q\rho_f C_{pf}}$ = dimensionless parameter

$B_R^* = \dfrac{E}{RT_R}\dfrac{\Delta T_{ad}}{T_R}\dfrac{UA_h}{q\rho_f C_{pf}}$ = dimensionless parameter

c_A = concentration of species A

C_{pf} = heat capacity per unit mass of fluid

$Da = \dfrac{k(T_o)V_r}{q}$ = Damkohler number at inlet conditions

$Da_R = \dfrac{k(T_R)V_r}{q}$ = Damkohler number at reaction conditions

E = activation energy

H = dimensionless overall heat transfer coefficient defined by Eq. 15b

$(-\Delta H_r)$ = heat of reaction

k = first order reaction rate constant

L = length of reactor tube

q = volumetric flow rate

R = universal gas constant

$St = \dfrac{UA_h}{q\rho_f C_{pf}}$ = Stanton number

t = state variable

T = absolute temperature

$\Delta T_{ad} = \dfrac{(-\Delta H_r)c_{A0}}{\rho_f C_{pf}}$ = adiabatic temperature rise

U = overall heat transfer coefficient

v = dimensionless parameter, defined by Eq. 81a

V_r = Volume of reactor

y = dimensionless temperature, defined by Eq. 5

y_R = ratio of reaction temperature to feed temperature, T_R/T_o

x = axial distance along reactor

Greek letters

β = dimensionless adiabatic temperature rise, defined by Eq. 5

β_R = dimensionless adiabatic temperature rise (reaction), defined by Eq. 75

$\beta^* = \dfrac{\Delta T_{ad}}{T_o} St$ = maximum possible preheating parameter

$\beta_R^* = \dfrac{\Delta T_{ad}}{T_R} St$ = maximum possible preheating parameter

$\hat{\beta}$ = maximum possible preheating parameter, defined by Eq. 61a

δ = dimensionless parameter, defined by Eq. 25

Δ = Frank-Kamenetskii number, defined by Eq. 33

χ = conversion of species A

γ = dimensionless activation energy, E/RT_o

γ_R = dimensionless activation energy (reaction), E/RT_R

θ = dimensionless temperature $= \gamma y$

ρ = density

ξ = dimensionless axial distance along reactor

Subscripts

d = preheat tube (downtube)

e = exit

ext = extinction

f = fluid

ig = ignition

o = inlet conditions

u = reactor tube (uptube)
R = reaction conditions

Literature Cited

Ampaya, J., and R. G. Rinker, "Design Correlations for Autothermal Reactors with Internal Countercurrent Heat Exchange," *Ind. Eng. Chem., Process Des. Dev.*, **16**, 63 (1977a).

Ampaya, J., and R. G. Rinker, "Autothermal Reactors with Internal Heat Exchange—I," *Chem. Eng. Sci.*, **32**, 1327 (1977b).

Aris, R., "On Stability Criteria of Chemical Reaction Engineering," *Chem. Eng. Sci.*, **24**, 149 (1969).

Baddour, R., P. Brian, B. Logeais, and J. Eymery, "Steady-State Simulation of an Ammonia Synthesis Converter," *Chem. Eng. Sci.*, **20**, 281 (1965).

Balakotaiah, V., and D. Luss, "Global Analysis of the Multiplicity Features of Multi-Reaction Lumped-Parameter Systems," *Chem. Eng. Sci.*, **39**, 865 (1984).

Eaton, B., and K. Gustafson, "Calculation of Critical Branching Points in Two-Parameter Bifurcation Problems," *J. Comp. Physics*, **50**, 171 (1983).

Frank-Kamenetskii, D. A., *Diffusion and Heat Transfer in Chemical Kinetics*, Plenum Press, New York (1969).

Inoue, H., and T. Komiya, "On the Stability of Autothermal Reactors," *Int. Chem. Eng.*, **8**, 749 (1968).

Inoue, H., "Static Thermal Stability of an Autothermal Reactor," *Chem. Eng. J. Japan*, **11**, 40 (1978).

Kaufmann, L. A., and H. Peterschek, "Modeling Vertech's Mile Long Reactor," *Chem. Eng. Sci.*, **41**, 685 (1986).

Kubicek, M., and M. Marek, *Computational Methods in Bifurcation Theory and Dissipative Structures*, Springer, New York (1983).

Lovo, M., H. A. Deans, and V. Balakotaiah, "Modeling and Simulation of Aqueous Hazardous Waste Oxidation in Deep Well Reactors," *Chem. Eng. Sci.*, **45**, 2703 (1990).

Lovo, M., "Steady State and Transient Behavior of a Deep Well Oxidation Reactor," PhD Thesis, University of Houston (1991).

Mukosei, V. I., L. M. Pis'men, and Y. I. Kharkats, "On Steady-State Regimes in Chemical Reactors with Internal, External and Combined Heat Exchange," *Int. Chem. Eng.*, **8**, 17 (1968).

Van Heerden, C., "Autothermic Processes: Properties and Reactor Design," *Ind. Eng. Chem.*, **45**, 1242 (1953).

Van Heerden, C., "The Character of the Stationary State of Exothermic Processes," *Chem. Eng. Sci.*, **8**, 133 (1958).

Witmer, G., V. Balakotaiah, and D. Luss, "Finding Singular Points of Two-Point Boundary Value Problems," *J. Comp. Physics*, **65**, 244 (1986).

Manuscript received Feb. 21, 1991, and revision received Nov. 18, 1991.